OPEN ACCESS

ORIGINAL ARTICLE

Microbiota-induced obesity requires farnesoid X receptor

Ava Parséus,[1] Nina Sommer,[1] Felix Sommer,[1] Robert Caesar,[1] Antonio Molinaro,[1] Marcus Ståhlman,[1] Thomas U Greiner,[1] Rosie Perkins,[1] Fredrik Bäckhed[1,2]

► Additional material is published online only. To view please visit the journal online (http://dx.doi.org/10.1136/gutjnl-2015-310283)

[1]Wallenberg Laboratory, Department of Molecular and Clinical Medicine, University of Gothenburg, Gothenburg, Sweden
[2]Section for Metabolic Receptology and Enteroendocrinology, Faculty of Health Sciences, Novo Nordisk Foundation Center for Basic Metabolic Research, University of Copenhagen, Copenhagen, Denmark

Correspondence to
Dr Fredrik Bäckhed, Wallenberg Laboratory, Sahlgrenska University Hospital, S-413 45 Gothenburg, Sweden; Fredrik.Backhed@wlab.gu.se

AP and NS contributed equally.

Received 3 July 2015
Revised 9 October 2015
Accepted 29 October 2015
Published Online First 6 January 2016

ABSTRACT

Objective The gut microbiota has been implicated as an environmental factor that modulates obesity, and recent evidence suggests that microbiota-mediated changes in bile acid profiles and signalling through the bile acid nuclear receptor farnesoid X receptor (FXR) contribute to impaired host metabolism. Here we investigated if the gut microbiota modulates obesity and associated phenotypes through FXR.

Design We fed germ-free (GF) and conventionally raised (CONV-R) wild-type and *Fxr*−/− mice a high-fat diet (HFD) for 10 weeks. We monitored weight gain and glucose metabolism and analysed the gut microbiota and bile acid composition, beta-cell mass, accumulation of macrophages in adipose tissue, liver steatosis, and expression of target genes in adipose tissue and liver. We also transferred the microbiota of wild-type and *Fxr*-deficient mice to GF wild-type mice.

Results The gut microbiota promoted weight gain and hepatic steatosis in an FXR-dependent manner, and the bile acid profiles and composition of faecal microbiota differed between *Fxr*−/− and wild-type mice. The obese phenotype in colonised wild-type mice was associated with increased beta-cell mass, increased adipose inflammation, increased steatosis and expression of genes involved in lipid uptake. By transferring the caecal microbiota from HFD-fed *Fxr*−/− and wild-type mice into GF mice, we showed that the obesity phenotype was transferable.

Conclusions Our results indicate that the gut microbiota promotes diet-induced obesity and associated phenotypes through FXR, and that FXR may contribute to increased adiposity by altering the microbiota composition.

Significance of this study

What is already known on this subject?

- The gut microbiota contributes to obesity
- The gut microbiota modulates farnesoid X receptor (FXR) signalling
- The gut microbiota metabolises a naturally occurring FXR antagonist

What are the new findings?

- The gut microbiota promotes obesity and associated diseases through FXR
- FXR alters the gut microbiota
- The altered gut microbiota contributes to the obese phenotype

How might it impact on clinical practice in the foreseeable future?

- Understanding how the gut microbiota modulates bile acids and signalling through FXR to modulate host metabolism may provide novel insights into how the microbiota can be targeted to prevent obesity.

INTRODUCTION

The gut microbiota is considered an environmental factor that modulates host metabolism, and recent evidence suggests that it contributes to the development of obesity and metabolic diseases. For example, the gut microbiota is altered in obese mice and humans[1–5] as well as in humans with type 2 diabetes.[6 7] Furthermore, germ-free (GF) mice have reduced adiposity and obesity, and transfer of microbiota from obese conventionally raised (CONV-R) mice to GF recipients has revealed that obesity is a transmissible trait through the microbiota.[8–11] Recent data also showed that faecal microbiota transplants from lean glucose-sensitive human donors improve insulin sensitivity in humans with the metabolic syndrome,[12] indicating that an altered gut microbiota may directly contribute to metabolic disease. However, little is known about the underlying mechanisms by which the gut microbiota affects host metabolism.

The gut microbiota metabolises dietary and host-derived molecules to produce bioactive components, which may play a role in host metabolism.[13] Bile acids, for example, are synthesised in the liver from cholesterol where they are conjugated to glycine (human) or taurine (mouse), and metabolised into secondary bile acids in the gut by the microbiota.[14 15] Bile acids are now recognised as signalling molecules that act through the nuclear receptor farnesoid X receptor (FXR) and the G-protein-coupled receptor TGR5 to regulate lipoprotein and glucose metabolism.[16–21] *Fxr*-deficient mice are protected against diet-induced obesity,[22] and studies in tissue-specific *Fxr*-deficient mice have revealed that intestinal FXR is required for the development of obesity, insulin resistance and non-alcoholic fatty liver disease in response to a high-fat diet (HFD).[23 24]

By comparing GF and CONV-R mice, we recently identified tauro-beta muricholic acid (TβMCA) as a potent FXR antagonist and showed that FXR suppression is alleviated by microbial

To cite: Parséus A, Sommer N, Sommer F, *et al*. *Gut* 2017;**66**:429–437.

metabolism of TβMCA to βMCA.[15] Similarly, modulation of the mouse gut microbiota using antibiotics or the antioxidant tempol increases the levels of TβMCA and suppresses FXR activity.[15 23 24] Furthermore, a recent study in human beings has shown that vancomycin treatment results in reduced Gram-positive bacteria, altered bile acid metabolism, and decreased insulin sensitivity.[25] These studies suggest that changes in the bile acid composition, and thus altered FXR signalling, may be a link between alterations in the microbiota and impaired host metabolism.

Here we use GF and *Fxr*−/− mice to test the hypothesis that the gut microbiota promotes obesity and associated phenotypes by activating FXR signalling. In addition, we investigate if FXR signalling contributes to obesity-associated phenotypes by altering the gut microbiota.

METHODS

Mice and diet

Male wild-type and whole-body *Fxr*-deficient GF and CONV-R mice on C57Bl/6 genetic background were maintained initially on autoclaved chow diet (LabDiet, Diet-5021-3-BG) and had access to diet and water *ad libitum*. GF mice were housed according to standard protocols in sterile flexible film isolators.[26] At 9–14 weeks of age, the mice were switched to irradiated vacuum-packed HFD (Harlan Laboratories, Diet TD.96132; 40% of energy from fat) *ad libitum* and then weighed in the isolators weekly for 10 weeks. Mice were housed under a 12 h light–dark cycle at 20±2°C and humidity range of 50±15%. All procedures were approved by the Ethics Committee on Animal Care and Use in Gothenburg, Sweden.

Glucose and insulin tolerance tests

An oral glucose tolerance test was performed after 10 weeks on HFD. Following a 4 h fast, mice were removed from the isolators and orally gavaged with 20% D-glucose (3 g/kg body weight). Blood was drawn from the tail vein at −30, 0, 15, 30, 60, 90 and 120 min and blood glucose levels were measured using a HemoCue glucometer. In addition, blood was collected from the tail vein at 0, 15 and 30 min for analysis of serum insulin levels using Ultra Sensitive Mouse Insulin ELISA (Crystal Chem).

An insulin tolerance test was performed in an independent cohort of mice after 10 weeks on HFD. Following a 4 h fast, mice were removed from the isolators and injected intraperitoneally with 0.25 U insulin/mL (0.75 mU/g body weight). Blood was drawn from the tail vein at −30, 0, 15, 30, 60, 90 and 120 min, and blood glucose levels were measured using a HemoCue glucometer.

Immunohistochemistry of pancreas and adipose tissue

Antibodies used are listed in online supplementary table S1. Paraffin-embedded pancreatic tissues fixed in 4% paraformaldehyde (HistoLab Products) were sectioned (6 µm). For the analysis of beta-cells, sections were stained with a guinea pig anti-insulin antibody and Vectastain ABC reagent followed by colour development using Vulcan Fast Red according to the manufacturer's protocol and counterstained with haematoxylin. Islet size and beta-cell area were quantified in two sections/mouse at least 200 µm apart from 5–7 mice/group using the software BioPix IQ Classic. Beta-cell mass was calculated by multiplying beta-cell area by the weight of the pancreas.

Paraffin-embedded epididymal white adipose tissue (WAT) was sectioned (6 µm) (HistoLab Products) and stained for MAC2 and crown-like structures as described previously.[27] The crown-like structures were manually counted with the software MIRAX Viewer in 14–20 images/histological section per mouse.

Quantitative real-time PCR

Approximately 30 mg epididymal WAT and liver were homogenised with TissueLyzer II (Qiagen) followed by total RNA extraction with RNeasy Mini Kit (Qiagen). Five hundred nanograms of pure cDNA were synthesised using the High Capacity cDNA Reverse Transcription Kit according to the manufacturer's protocol (Applied Biosystems). The cDNA was diluted 7× before subsequent reactions. For qRT-PCR reactions, IQ SYBR Green Supermix (Bio-Rad) was used at an end volume of 25 µL, and 0.9 µM of gene-specific primers were added (see online supplementary table S2). Gene-specific primers were normalised to the housekeeping gene L32. Each primer set was verified by analysis of their melt curves, and the assays were performed in a 7900HT Fast Real-Time PCR System (Applied Biosystems) or CFX96 Real System (Bio-Rad). The $\Delta\Delta C_T$ analysis method was used to analyse the reactions.

Liver lipid analysis

Snap frozen tissue was placed into 2 mL Sarstedt tubes loaded with six zirconium oxide beads (3 mm) (Retsch). Tissue was homogenised for 10 min at 25 Hz in 500 µL methanol using a Mixer Mill 301 instrument (Retsch). Lipids were then extracted using the Folch method.[28] Cholesteryl esters and triglycerides were quantified using direct infusion/mass spectrometry as described previously.[29]

Alanine transaminase analysis

Alanine transaminase (ALT) activity was measured in 20 µL vena cava sera from n = 5–8 mice/group using EnzyChrom ALT Assay Kit (Bioassay Systems). The samples were added to CFX96 Real System plates (Bio-Rad), and the ALT activity was thereafter determined according to colorimetric measurement using OD read at 340 nm.

Microbiota analysis

Total DNA was isolated from faecal samples after 10 weeks of HFD feeding as described previously.[30–32] The V4 region of the 16S rDNA gene was amplified using barcoded primers, and sequencing was performed using MiSeq Gene & Small Genome Sequencer from Illumina. Reads were analysed using the MacQIIME V.1.8 software package (http://www.wernerlab.org/software/macqiime[33]) as described previously.[34] Briefly, operational taxonomic units were picked using UCLUST, and taxonomic assignments were made using the Ribosomal Database Project. Singletons, chimeric sequences and those that failed to align with PyNAST were removed. Relative abundance, Unifrac α and beta diversity were calculated and phylogeny constructed using UPGMA (Unweighted Pair Group Method with Arithmetic Mean). Significance of differences in abundances was calculated using t test and false discovery-rate correction. Linear discriminant analysis (LDA) effect size (LEfSe) analysis was performed using standard parameters ($p<0.05$ and LDA score 2.0) as described in ref. 35.

Bile acid analysis

Bile acids were extracted from vena cava serum (n=5–9 mice/group) and from caecal content (n=3–9 mice/group) after 10 weeks of HFD using 10 volumes of methanol-containing internal standards. After vigorous mixing for 5 min, the samples were centrifuged at 22 000 *g* for 10 min. The supernatant

was removed and diluted 10 times with water/methanol (1:1). The samples were then analysed using ultra-performance liquid chromatography–tandem mass spectrometry (UPLC-MS/MS).[36]

Microbiota transfer experiments

Caecal content was collected from wild-type and *Fxr*−/− mice on HFD for 10 weeks; at the time of collection, mice were fed and the light had been on for 3–5 h. GF C57BL/6J mice aged 9 weeks were gavaged with the caecal content and transferred to HFD for 10 weeks. Mice were weighed weekly. After 10 weeks of HFD, body fat was assessed by MRI and an oral glucose tolerance test was performed in these mice.

Statistical analysis

Data are represented as mean ±SEM. Multiple groups were analysed by two-way ANOVA followed by Bonferroni post hoc test; detailed information can be found in online supplementary table S3. Statistical differences in bile acids between wild-type and *Fxr*−/− mice were determined using two-tailed, unpaired, FDR-corrected Student's t test. GraphPad Prism 5 software was used for two-way ANOVA and t test. The effect of *Fxr* knockout on weight gain over time was analysed by using a mixed two-way ANOVA test in R. In this test, the genotype was considered as a between-sample variable and time as a within-sample variable.

RESULTS

Effect of the gut microbiota on diet-induced obesity and glucose metabolism is reduced in Fxr−/− mice

Previous studies have shown that GF mice are protected against diet-induced obesity and have improved glucose metabolism compared with their colonised counterparts,[9 37 38] but the underlying mechanisms are unknown. Here, we fed GF and CONV-R wild-type and *Fxr*−/− mice a HFD for 10 weeks to investigate whether the gut microbiota affects diet-induced weight gain and glucose metabolism through FXR. As expected, CONV-R wild-type mice gained significantly more weight than GF wild-type mice after 10 weeks on a HFD (figure 1A). The increased obesity in CONV-R versus GF wild-type mice was associated with increased fasting glucose and insulin levels and impaired glucose and insulin tolerance (figure 1B–F). In the absence of intact FXR signalling, the gut microbiota did not affect weight gain (figure 1A). However, the presence of gut microbiota in *Fxr*-deficient mice resulted in increased fasting glucose levels and impaired oral glucose tolerance; these changes were similar to the microbiota-induced changes observed in wild-type mice (figure 1B, C). By contrast, the presence of gut microbiota did not affect fasting insulin, insulin release after glucose administration nor insulin tolerance in *Fxr*-deficient mice (figure 1D–F). Insulin staining of tissue sections from the pancreas demonstrated that islet size and beta-cell mass were greater in CONV-R versus GF wild-type mice but were not affected by the presence of a microbiota in *Fxr*−/− mice (figure 1G–I).

We noted that the gut microbiota did not significantly affect FXR expression in the small intestine and liver, tissues where FXR is most abundantly expressed, or in WAT (data not shown).

As expected, we found that obese CONV-R wild-type mice had increased adiposity and larger adipocytes compared with GF counterparts after 10 weeks on a HFD; this difference was abolished in *Fxr*−/− mice (figure 2A). In agreement, we showed that the number of crown-like structures (which indicate accumulation of macrophages around necrotic adipocytes) and the expression of the macrophage markers *Emr1* (which encodes the protein F4/80), *Saa3* and *Tnfa* (which encode proinflammatory cytokines) and *Ccl2* (which promotes macrophage infiltration into WAT[39]) were markedly increased by the microbiota in adipose tissue from wild-type but not *Fxr*−/− mice (figure 2B–F).

These data suggest that microbiota-induced obesity is associated with increased macrophage infiltration and that this process requires functional FXR signalling.

Effect of the gut microbiota on hepatic steatosis is reduced in Fxr−/− mice

Obesity is associated with increased hepatic steatosis, which correlates with insulin resistance.[40 41] Because FXR has been demonstrated to have a large impact on hepatic lipid metabolism,[16] we investigated whether the gut microbiota induces steatosis through activating FXR signalling. Quantification using direct infusion/mass spectrometry showed higher levels of triglycerides, saturated triglycerides and cholesteryl esters in livers of CONV-R wild-type mice compared with GF mice after 10 weeks on a HFD (figure 3A–C). The increased hepatic steatosis in CONV-R wild-type mice was also associated with elevated ALT levels (figure 3D), indicating increased hepatic inflammation. By contrast, the presence of a gut microbiota did not promote hepatic steatosis or increased ALT activity in *Fxr*−/− mice (figure 3A–D).

We next investigated the effect of the microbiota on FXR-regulated genes in the liver that could potentially contribute to hepatic steatosis. The increased lipid accumulation in CONV-R wild-type mice after high-fat feeding could not be explained by increased expression of lipogenic genes such as *Fas* and *Acc1* (see online supplementary figure S1A,B) nor by reduced expression of genes involved in fatty acid oxidation such as *Ppara*, *Acox1* and *Cpt1a* (see online supplementary figure S1C–E). However, we found significant upregulation of the fatty acid transporter *Cd36* as well as *Apoc2* and *Vldlr* in liver from CONV-R versus GF wild-type mice or *Fxr*−/− mice with or without a microbiota (figure 3E–G). These data suggest that the microbiota may promote diet-induced hepatic steatosis at least partly through activation of FXR-regulated fatty acid and lipoprotein uptake genes in the liver.

FXR alters bile acid and gut microbiota composition

The gut microbiota and FXR have profound effects on bile acid metabolism,[14–16] and here we used ultra-performance liquid chromatography–MS/MS to quantify serum and caecal bile acids from CONV-R and GF wild-type and *Fxr*−/− counterparts. We found that the bile acid composition in serum and caecum of GF mice was dominated by TβMCA and was not affected by *Fxr* genotype (see online supplementary figure S2A,B). By contrast, differences in the bile acid profiles of serum were observed when we compared CONV-R wild-type and *Fxr*−/− mice: CONV-R *Fxr*-deficient mice had a significantly higher proportion of TβMCA (see online supplementary figure S2A), suggesting reduced capacity to deconjugate bile acids. Caecal bile acids in CONV-R mice were predominantly deconjugated and dominated by secondary bile acids (see online supplementary figure S2B), as previously demonstrated in mice on chow diet.[15] Consistent with the higher level of TβMCA in the serum of CONV-R *Fxr*−/− mice, these mice had a trend towards higher caecal levels of βMCA compared with CONV-R wild-type mice (see online supplementary figure S2B), further suggesting reduced capacity to metabolise bile acids in the absence of functional FXR signalling.

The altered serum bile acid profile was associated with reduced hepatic expression of *Cyp7a1* in CONV-R wild-type

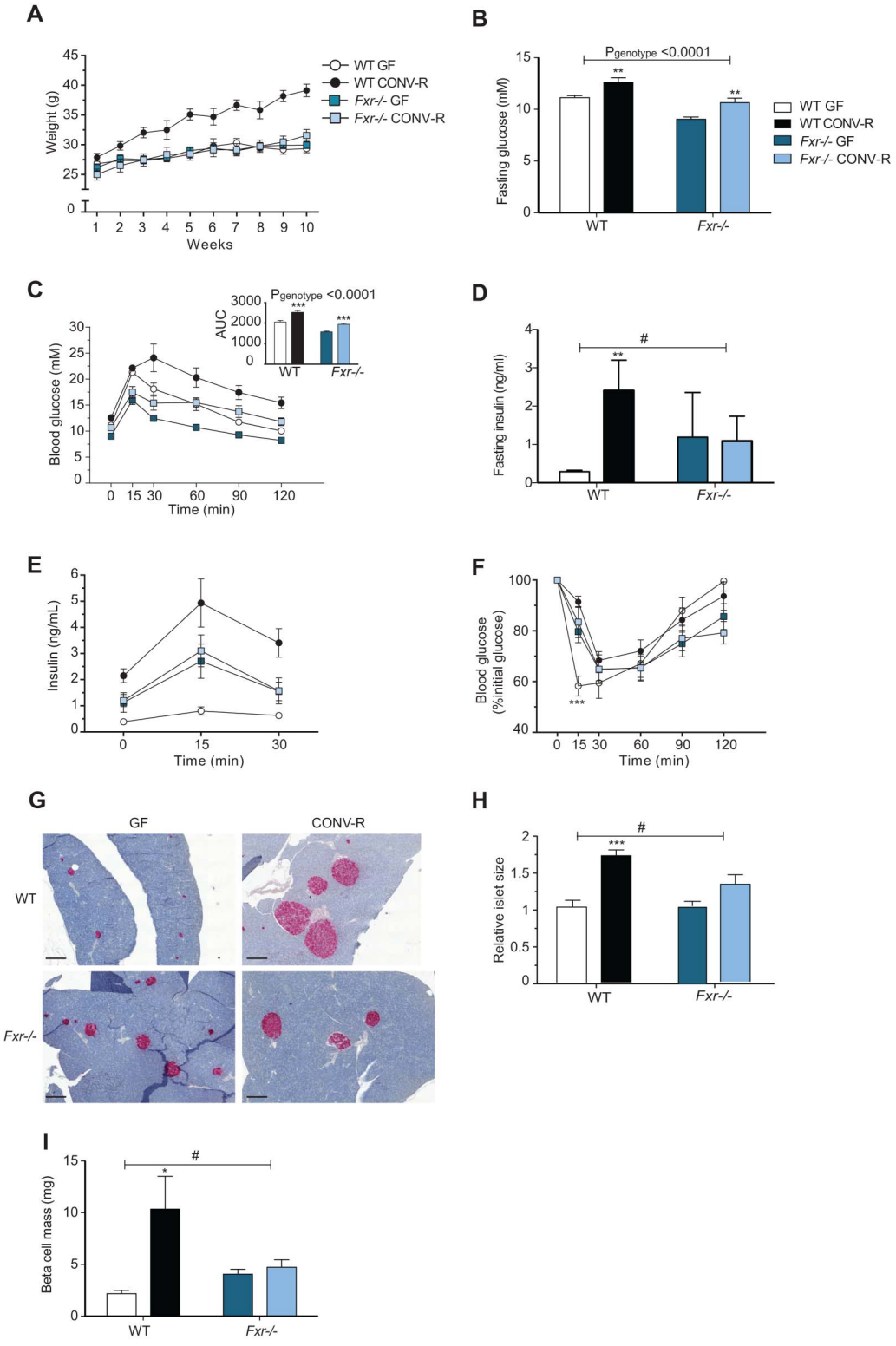

Figure 1 Farnesoid X receptor (FXR) and the gut microbiota regulate development of diet-induced obesity. (A) Weight gain of 9-week to 14-week old germ-free (GF) and CONV-R wild-type and *Fxr−/−* male mice on a high-fat diet (HFD) for 10 weeks (n=7–14 mice per group). (B) Fasting glucose levels, (C) oral glucose tolerance test, (D) fasting insulin levels and (E) blood insulin levels during the first 30 min of the oral glucose tolerance test in mice after 10 weeks on a HFD (n=6–7 mice per group). (F) Insulin tolerance test in mice after 10 weeks on a HFD (n=10–11 mice per group). (G) Pancreatic sections stained for insulin (red) and haematoxylin (blue) from mice after 10 weeks on a HFD. Scale bars, 200 μm. (H) Islet size (relative to GF wild-type) in mice after 10 weeks of HFD (n=5–9 mice per group). (I) Beta-cell mass in mice after 10 weeks on a HFD (n=5–8 mice per group). Mean values±SEM are plotted; *p<0.05, **p<0.01, ***p<0.001 versus GF mice of same genotype; #significant for genotype–colonisation interaction.

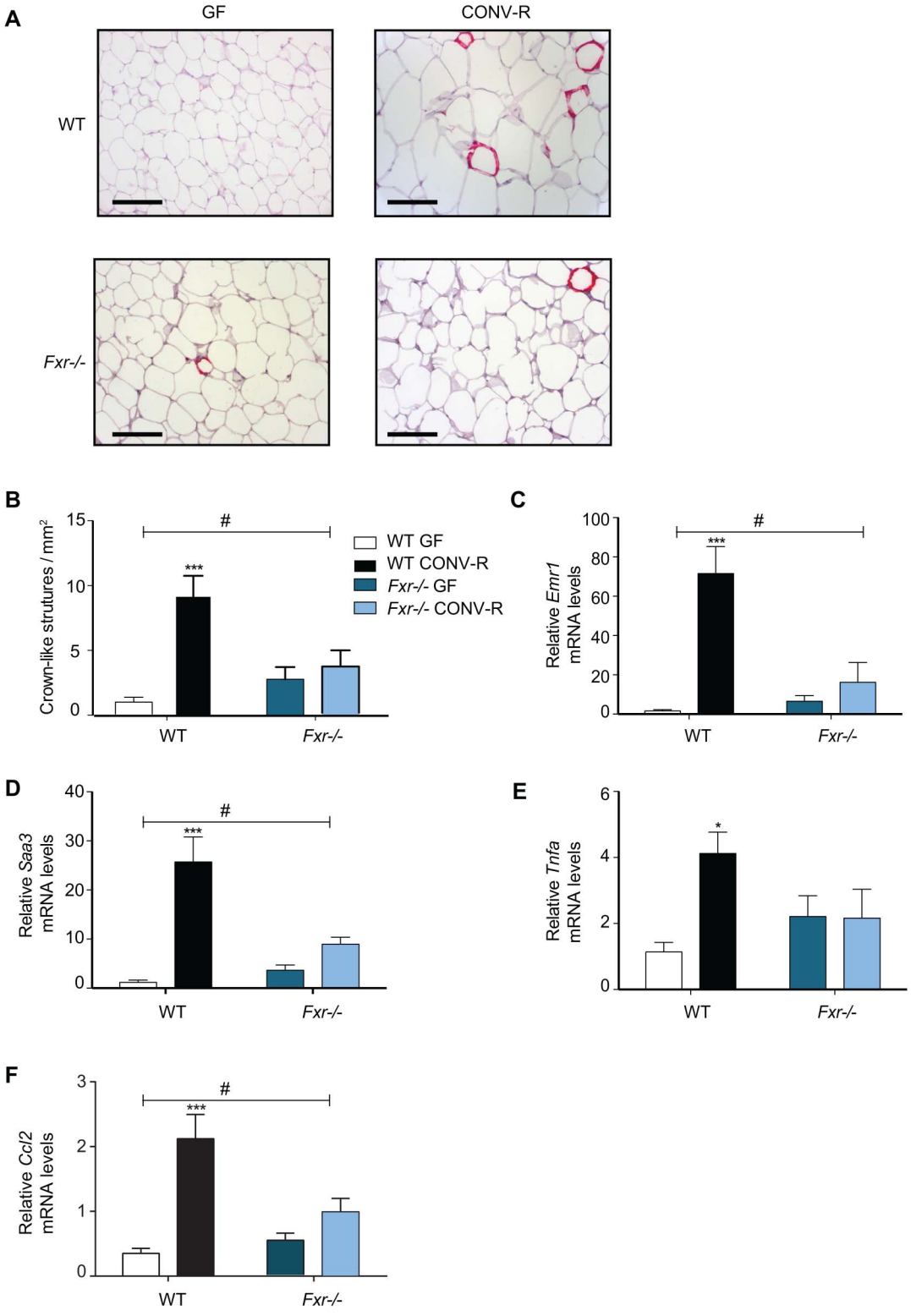

Figure 2 Gut microbiota increases crown-like structures and expression of proinflammatory markers in white adipose tissue (WAT) through farnesoid X receptor (FXR). (A) Representative MAC-2 immunostaining of WAT from germ-free (GF) and CONV-R wild-type and *Fxr−/−* male mice on a high-fat diet (HFD) for 10 weeks. Scale bars, 100 μm. (B) Quantification of crown-like structures (n=6–7 mice per group). (C–F) qPCR analysis of *Emr1*, *Saa3*, *Tnfα* and *Ccl2* expression in WAT from mice after 10 weeks on a HFD (n=4–9 mice per group). Mean values±SEM are plotted; *p<0.05, **p<0.01, ***p<0.001 versus GF of same genotype; #significant for genotype–colonisation interaction.

mice compared with the other groups; by contrast genotype, but not microbiota, affected *Cyp8b1* expression (see online supplementary figure S3A, B).

To investigate whether the metabolic differences between CONV-R wild-type and *Fxr−/−* mice were associated with an altered gut microbiota, we extracted genomic DNA

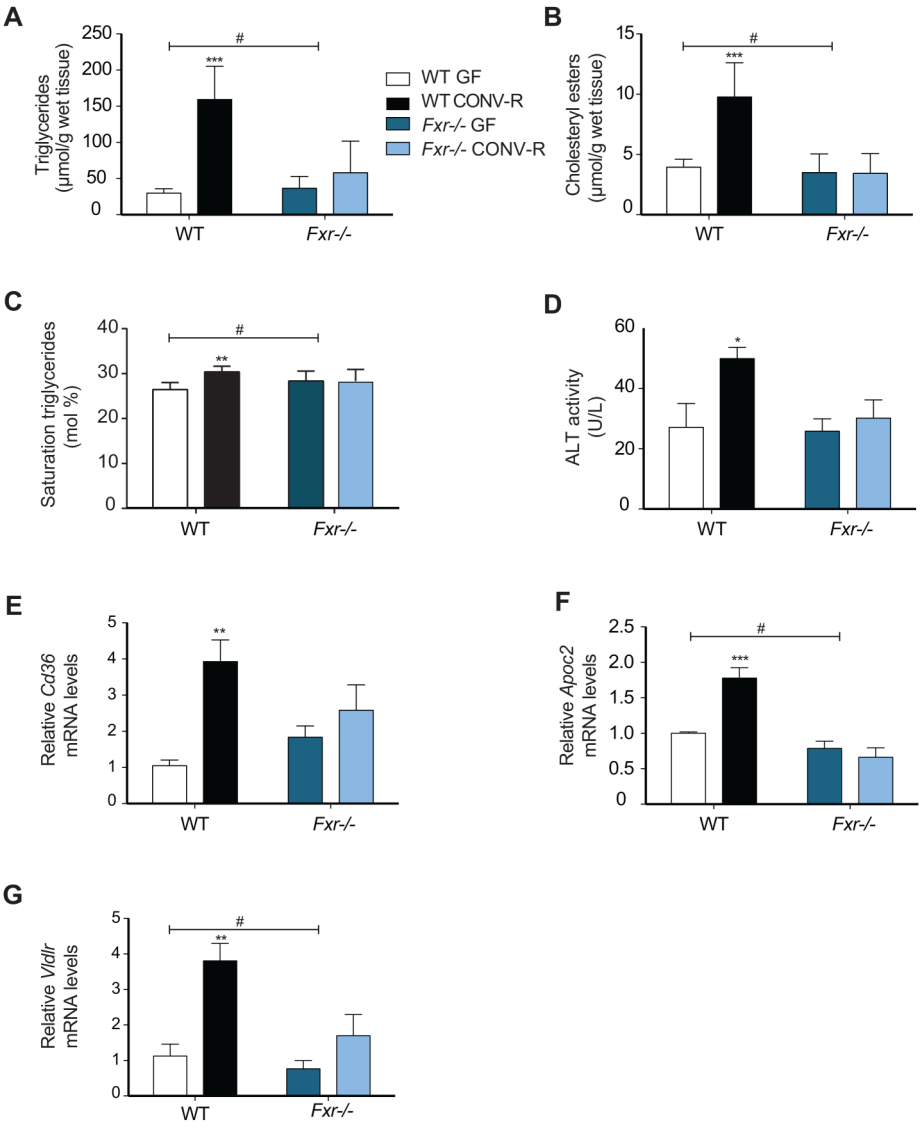

Figure 3 Gut microbiota increases hepatic steatosis and expression of genes involved in lipoprotein uptake through farnesoid X receptor (FXR). (A) Quantification of triglycerides, (B) saturated triglycerides and (C) cholesteryl esters in livers from germ-free (GF) and CONV-R wild-type and *Fxr*−/− male mice after 10 weeks on a high-fat diet (HFD) (n=4–9 mice per group). (D) Alanine transaminase (ALT) levels in the serum of mice after 10 weeks on a HFD (n=5–8 mice per group). (E–G) qPCR analysis of *Cd36*, *Apoc2 and Vldlr* expression in livers from mice after 10 weeks on a HFD (n=4–9 mice per group). Mean values ±SEM are plotted; *p<0.05, **p<0.01, ***p<0.001 versus GF of same genotype; #significant for genotype–colonisation interaction.

from faecal contents of these mice and sequenced the 16S rRNA gene using MiSeq. Unweighted UniFrac analysis (qualitative; not sensitive to abundance of taxa) showed a clear separation between CONV-R wild-type and *Fxr*−/− mice (figure 4A). We observed decreased levels of Firmicutes and increased levels of Bacteroidetes in CONV-R *Fxr*−/− compared with wild-type mice after 10 weeks on a HFD (figure 4B, C). LEfSe also indicated that genera belonging to Firmicutes, Epsilon- and Gamma proteobacteria were increased in CONV-R wild-type mice and that genera belonging to Bacteroidia were increased in CONV-R *Fxr*−/− mice (figure 4D).

Altered gut microbiota from Fxr−/− mice modulates obesity and glucose metabolism on transfer to GF wild-type mice

Previous studies have shown that the obesity phenotype can be transferred by transplanting the microbiota from obese mice into GF recipients.[3 10 11] To assess whether the altered gut microbiota of CONV-R *Fxr*−/− mice could contribute to the metabolic differences between CONV-R wild-type and *Fxr*−/− mice, we therefore colonised GF wild-type mice with the caecal microbiota from HFD-fed CONV-R *Fxr*−/− or wild-type mice. After 10 weeks on a HFD, mice colonised with the CONV-R *Fxr*−/− microbiota [CONV-D(*Fxr*−/−)] gained less weight than mice that were colonised with the CONV-R wild-type microbiota [CONV-D(WT)] (figure 4E). Furthermore, MRI analysis showed that adiposity was significantly lower in CONV-D(*Fxr*−/−) mice than in CONV-D(WT) mice (figure 4F). As we had shown that *Fxr*−/− mice had improved oral glucose tolerance compared with their wild-type counterparts ($p<0.001$; figure 1C), we investigated whether this effect could also be transferred by transplanting the microbiota. Indeed, we showed that glucose tolerance was improved in CONV-D(*Fxr*−/−) mice compared with CONV-D(WT) mice after 10 weeks on a HFD (figure 4G). These data suggest that the altered gut microbiota in HFD-fed CONV-R *Fxr*-deficient mice may at least partly contribute to some of the beneficial metabolic effects observed in these mice.

DISCUSSION

To investigate whether the gut microbiota promotes diet-induced obesity and associated phenotypes through an FXR-dependent mechanism, we rederived *Fxr*-deficient mice as GF and compared them with CONV-R counterparts. We found that the gut microbiota promoted diet-induced obesity, adipose inflammation and liver steatosis in a strict FXR-dependent fashion. Furthermore, we showed that *Fxr*-deficient mice had an altered bile acid and gut microbiota composition. By transferring the microbiota from wild-type and *Fxr*−/− CONV-R mice

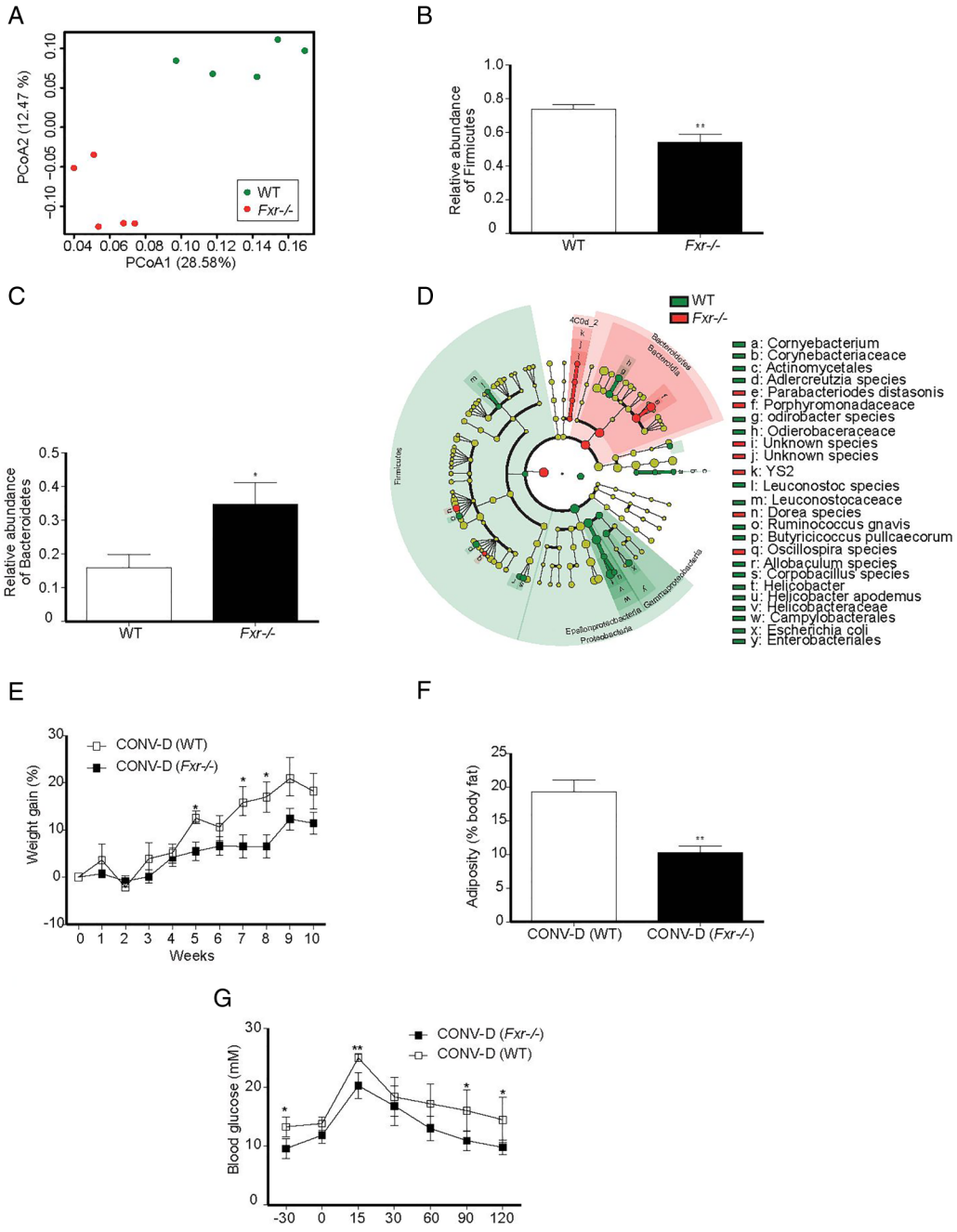

Figure 4 Farnesoid X receptor (FXR) signalling alters the gut microbiota leading to modulation of glucose metabolism. (A) Principal coordinates analysis plot of unweighted Unifrac distances and (B–C) relative abundance of Firmicutes and Bacteroidetes in faeces of CONV-R wild-type or *Fxr* −/− mice on a high-fat diet (HFD) for 10 weeks (n=4–5 mice per group). (D) Cladogram generated from LEfSe analysis showing the most differentially abundant taxa enriched in microbiota from wild-type (green) and *Fxr*−/− (red) mice. (E) Weight gain, (F) fat content as a percentage of body weight and (G) oral glucose tolerance test in mice conventionalised with caecal microbiota from wild-type mice [CONV-D (WT)] or from *Fxr*−/− mice [CONV-D (*Fxr*−/−)] and fed a HFD for 10 weeks (n=5 mice/group). Mean values±SEM are plotted; *p<0.05, **p<0.01, ***p<0.001.

to GF recipients, we showed that the altered microbiota partly contributed to the improved metabolic profile of *Fxr*-deficient mice.

As expected, lean GF wild-type mice had low fasting insulin levels and beta-cell mass, and exhibited improved insulin tolerance in comparison with obese CONV-R mice. Although the phenotypes of GF and CONV-R *Fxr*-deficient mice were mostly similar, highlighting microbial signalling through FXR, we noted that GF *Fxr*-deficient mice had improved fasting glucose and glucose tolerance compared with CONV-R *Fxr*−/− mice. Interestingly, the presence of a gut microbiota resulted in elevated fasting glucose levels without an effect on fasting insulin levels in *Fxr*-deficient mice. Although this could potentially be explained by CONV-R *Fxr*−/− mice having a higher degree of insulin resistance than GF *Fxr*−/− mice, this did not translate into impaired insulin tolerance in CONV-R *Fxr*−/− mice. However, it should be noted that an insulin tolerance test is mainly a reflection of overall insulin sensitivity (ie, muscle glucose usage), and cannot take into account hepatic insulin resistance. Thus, one explanation of the discrepancy between glycaemic and insulinaemic profiles could be linked to hepatic insulin resistance.

Our observation that the gut microbiota induced liver steatosis in response to a HFD in an FXR-dependent manner is in agreement with a recent finding showing that antibiotic treatment reduces steatosis through FXR signalling.[24] We also observed increased expression of *Cd36*, *Apoc2* and *Vldlr* in liver from wild-type mice but not *Fxr*-deficient counterparts. All three genes are associated with lipoprotein uptake,[42–44] which may explain increased steatosis, which could not be attributed to increased expression of lipogenic genes or reduced expression of genes involved in fatty acid oxidation. Furthermore, *Vldlr*−/− mice have been shown to be protected against developing steatosis[45] and diet-induced obesity.[46]

It is well known that the gut microbiota affects bile acid metabolism,[15 23] and changes in the bile acid profile may partly explain the increased adiposity in CONV-R versus GF wild-type mice. In the absence of the microbiota, the serum bile acid profile was not affected by *Fxr* genotype and was dominated by TβMCA, highlighting the importance of the microbiota to promote bile acid diversity. By contrast, in the presence of a microbiota, *Fxr* deficiency had profound effects on the serum bile acid profile, which may be a consequence of altered gut microbial communities and/or increased production of bile acids. Bile acids can directly modulate bacterial growth and microbial ecology in the gut.[47 48] In addition, bile acids can indirectly modulate the gut microbiota by promoting FXR-induced expression of genes producing antimicrobial agents such as *Nos2* in the small intestine.[49] Thus, an altered bile acid profile may potentially contribute to the alterations in host metabolism observed in *Fxr*-deficient versus wild-type mice by modifying the microbiota composition. To test this hypothesis, we compared the gut microbiota of wild-type and *Fxr*-deficient mice. We showed that the gut microbiota of *Fxr*-deficient mice was characterised by a phylum-wide increase in Bacteroidetes and phylum-wide reduction of Firmicutes. Similar alterations have previously been associated with protection against obesity.[1 3] Importantly, we also showed that the transfer of the microbiota from HFD-fed *Fxr*-deficient mice to GF wild-type mice resulted in less fat mass gain and improved glucose metabolism compared with mice that were colonised with microbiota from HFD-fed wild-type mice. Thus, our findings suggest that the altered gut microbiota in HFD-fed *Fxr*-deficient mice may directly contribute to the lean phenotype.

In conclusion, our results support the concept that the gut microbiota promotes diet-induced obesity and associated phenotypes through effects on the bile acid profile and altered FXR signalling. Furthermore, our findings indicate that FXR may also contribute to increased adiposity by shifting the gut microbiota to a more obesogenic configuration. Thus, manipulation of the gut microbiota and/or FXR signalling may reveal novel ways to treat metabolic disease. However, the precise role of FXR in host metabolism is complex, and conflicting studies have reported that intestinal FXR signalling promotes[23] or protects against[50] obesity. Taken together, although it is clear that the gut microbiota and FXR regulate host metabolism, the underlying molecular mechanisms require further investigation.

Acknowledgements We thank Carina Arvidsson and Anna Hallén for superb technical assistance, the genomics core facility at University of Gothenburg for 16S sequencing, Valentina Tremaroli and Rozita Akrami for assisting with microbiota analysis and Frank Gonzalez for providing *Fxr*−/− mice.

Contributors FB conceived and designed the study; AP, NS, FS, RC, AM, MS and TG performed experiments; AP, NS, FS, RP and FB analysed and interpreted the data; AP, NS, RP and FB wrote the paper; All authors commented and approved the final manuscript.

Funding This work was supported by the Human Frontier of Science Program (RGY64/2008), Swedish Research Council, NovoNordisk Foundation, Torsten Söderberg's Foundation, Ragnar Söderberg's Foundation, Swedish Diabetes Foundation, Swedish Heart Lung Foundation, IngaBritt och Arne Lundbergs Foundation, Knut and Alice Wallenberg Foundation, Swedish Foundation for Strategic Research, the EU-funded project ETHERPATHS (FP7-KBBE-222639, www.etherpaths.org), Åke Wiberg, Magnus Bergvall, Lars Hierta's, Nanna Svartz, Fredrik and Ingrid Thurings Foundations and LUA-ALF grants from Sahlgrenska University Hospital. FB is a recipient of ERC consolidator Grant 2013 (European Research Council, Consolidator grant 615362-METABASE).

Competing interests FB is the founder and share holder of Metabogen AB.

Provenance and peer review Not commissioned; externally peer reviewed.

Data sharing statement Sequencing data will be made available in public databases.

REFERENCES

1 Ley RE, Bäckhed F, Turnbaugh P, *et al*. Obesity alters gut microbial ecology. *Proc Natl Acad Sci USA* 2005;102:11070–5.
2 Ley RE, Turnbaugh PJ, Klein S, *et al*. Microbial ecology: human gut microbes associated with obesity. *Nature* 2006;444:1022–3.
3 Turnbaugh PJ, Bäckhed F, Fulton L, *et al*. Diet-induced obesity is linked to marked but reversible alterations in the mouse distal gut microbiome. *Cell Host Microbe* 2008;3:213–23.
4 Le Chatelier E, Nielsen T, Qin J, *et al*. Richness of human gut microbiome correlates with metabolic markers. *Nature* 2013;500:541–6.
5 Turnbaugh PJ, Hamady M, Yatsunenko T, *et al*. A core gut microbiome in obese and lean twins. *Nature* 2009;457:480–4.
6 Karlsson FH, Tremaroli V, Nookaew I, *et al*. Gut metagenome in European women with normal, impaired and diabetic glucose control. *Nature* 2013;498:99–103.
7 Qin J, Li Y, Cai Z, *et al*. A metagenome-wide association study of gut microbiota in type 2 diabetes. *Nature* 2012;490:55–60.
8 Bäckhed F, Ding H, Wang T, *et al*. The gut microbiota as an environmental factor that regulates fat storage. *Proc Natl Acad Sci USA* 2004;101:15718–23.
9 Bäckhed F, Manchester JK, Semenkovich CF, *et al*. Mechanisms underlying the resistance to diet-induced obesity in germ-free mice. *Proc Natl Acad Sci USA* 2007;104:979–84.
10 Turnbaugh PJ, Ley RE, Mahowald MA, *et al*. An obesity-associated gut microbiome with increased capacity for energy harvest. *Nature* 2006;444:1027–31.
11 Ridaura VK, Faith JJ, Rey FE, *et al*. Gut microbiota from twins discordant for obesity modulate metabolism in mice. *Science* 2013;341:1241214.
12 Vrieze A, Van Nood E, Holleman F, *et al*. Transfer of intestinal microbiota from lean donors increases insulin sensitivity in individuals with metabolic syndrome. *Gastroenterology* 2012;143:913–6.e7.
13 Tremaroli V, Backhed F. Functional interactions between the gut microbiota and host metabolism. *Nature* 2012;489:242–9.
14 Midtvedt T. Microbial bile acid transformation. *Am J Clin Nutr* 1974;27:1341–7.
15 Sayin SI, Wahlström A, Felin J, *et al*. Gut microbiota regulates bile acid metabolism by reducing the levels of tauro-beta-muricholic acid, a naturally occurring FXR antagonist. *Cell Metabolism* 2013;17:225–35.
16 Sinal CJ, Tohkin M, Miyata M, *et al*. Targeted disruption of the nuclear receptor FXR/BAR impairs bile acid and lipid homeostasis. *Cell* 2000;102:731–44.
17 Makishima M, Okamoto AY, Repa JJ, *et al*. Identification of a nuclear receptor for bile acids. *Science* 1999;284:1362–5.
18 Parks DJ, Blanchard SG, Bledsoe RK, *et al*. Bile acids: natural ligands for an orphan nuclear receptor. *Science* 1999;284:1365–8.
19 Wang H, Chen J, Hollister K, *et al*. Endogenous bile acids are ligands for the nuclear receptor FXR/BAR. *Mol Cell* 1999;3:543–53.
20 Maruyama T, Miyamoto Y, Nakamura T, *et al*. Identification of membrane-type receptor for bile acids (M-BAR). *Biochem Biophys Res Commun* 2002;298:714–9.
21 Kawamata Y, Fujii R, Hosoya M, *et al*. A G protein-coupled receptor responsive to bile acids. *J Biol Chem* 2003;278:9435–40.
22 Prawitt J, Abdelkarim M, Stroeve JH, *et al*. Farnesoid X receptor deficiency improves glucose homeostasis in mouse models of obesity. *Diabetes* 2011;60:1861–71.
23 Li F, Jiang C, Krausz KW, *et al*. Microbiome remodelling leads to inhibition of intestinal farnesoid X receptor signalling and decreased obesity. *Nat Commun* 2013;4:2384.

24 Jiang C, Xie C, Li F, *et al*. Intestinal farnesoid X receptor signaling promotes nonalcoholic fatty liver disease. *J Clin Invest* 2015;125:386–402.
25 Vrieze A, Out C, Fuentes S, *et al*. Impact of oral vancomycin on gut microbiota, bile acid metabolism, and insulin sensitivity. *J Hepatol* 2014;60:824–31.
26 Arvidsson C, Hallén A, Bäckhed F. *Generating and analyzing germ-free mice. Current protocols in mouse biology*. John Wiley & Sons, Inc., 2011.
27 Caesar R, Reigstad CS, Backhed HK, *et al*. Gut-derived lipopolysaccharide augments adipose macrophage accumulation but is not essential for impaired glucose or insulin tolerance in mice. *Gut* 2012;61:1701–7.
28 Folch J, Lees M, Sloane Stanley GH. A simple method for the isolation and purification of total lipides from animal tissues. *J Biol Chem* 1957;226: 497–509.
29 Stahlman M, Fagerberg B, Adiels M, *et al*. Dyslipidemia, but not hyperglycemia and insulin resistance, is associated with marked alterations in the HDL lipidome in type 2 diabetic subjects in the DIWA cohort: impact on small HDL particles. *Biochim Biophys Acta* 2013;1831:1609–17.
30 Yu Z, Morrison M. Improved extraction of PCR-quality community DNA from digesta and fecal samples. *BioTechniques* 2004;36:808–12.
31 Salonen A, Nikkila J, Jalanka-Tuovinen J, *et al*. Comparative analysis of fecal DNA extraction methods with phylogenetic microarray: effective recovery of bacterial and archaeal DNA using mechanical cell lysis. *J Microbiol Methods* 2010;81:127–34.
32 Nylund L, Heilig HG, Salminen S, *et al*. Semi-automated extraction of microbial DNA from feces for qPCR and phylogenetic microarray analysis. *J Microbiol Methods* 2010;83:231–5.
33 Caporaso JG, Kuczynski J, Stombaugh J, *et al*. QIIME allows analysis of high-throughput community sequencing data. *Nat Methods* 2010;7:335–6.
34 Sommer F, Adam N, Johansson MEV, *et al*. Altered mucus glycosylation in core 1 O-glycan-deficient mice affects microbiota composition and intestinal architecture. *PLoS One* 2014;9:e85254.
35 Segata N, Izard J, Waldron L, *et al*. Metagenomic biomarker discovery and explanation. *Genome Biol* 2011;12:R60.
36 Garcia-Canaveras JC, Donato MT, Castell JV, *et al*. Targeted profiling of circulating and hepatic bile acids in human, mouse, and rat using a UPLC-MRM-MS-validated method. *J Lipid Res* 2012;53:2231–41.
37 Ding S, Chi MM, Scull BP, *et al*. High-fat diet: bacteria interactions promote intestinal inflammation which precedes and correlates with obesity and insulin resistance in mouse. *PLoS One* 2010;5:e12191.
38 Rabot S, Membrez M, Bruneau A, *et al*. Germ-free C57BL/6J mice are resistant to high-fat-diet-induced insulin resistance and have altered cholesterol metabolism. *FASEB J* 2010;24:4948–59.
39 Caesar R, Tremaroli V, Kovatcheva-Datchary P, *et al*. Crosstalk between gut microbiota and dietary lipids aggravates WAT inflammation through TLR signaling. *Cell Metab* 2015;22:658–68.
40 Yki-Jarvinen H. Fat in the liver and insulin resistance. *Ann Med* 2005;37:347–56.
41 Marchesini G, Brizi M, Morselli-Labate AM, *et al*. Association of nonalcoholic fatty liver disease with insulin resistance. *Am J Med* 1999;107:450–5.
42 Niemeier A, Gàfvels M, Heeren J, *et al*. VLDL receptor mediates the uptake of human chylomicron remnants in vitro. *J Lipid Res* 1996;37:1733–42.
43 Guo GL, Santamarina-Fojo S, Akiyama TE, *et al*. Effects of FXR in foam-cell formation and atherosclerosis development. *Biochim Biophys Acta* 2006;1761:1401–9.
44 Calkin AC, Tontonoz P. Transcriptional integration of metabolism by the nuclear sterol-activated receptors LXR and FXR. *Nat Rev Mol Cell Biol* 2012;13:213–24.
45 Jo H, Choe SS, Shin KC, *et al*. Endoplasmic reticulum stress induces hepatic steatosis via increased expression of the hepatic very low-density lipoprotein receptor. *Hepatology* 2013;57:1366–77.
46 Goudriaan JR, Tacken PJ, Dahlmans VEH, *et al*. Protection from obesity in mice lacking the VLDL receptor. *Arterioscler Thromb Vasc Biol* 2001;21:1488–93.
47 Binder HJ, Filburn B, Floch M. Bile acid inhibition of intestinal anaerobic organisms. *Am J Clin Nutr* 1975;28:119–25.
48 Islam KB, Fukiya S, Hagio M, *et al*. Bile acid is a host factor that regulates the composition of the cecal microbiota in rats. *Gastroenterology* 2011;141:1773–81.
49 Inagaki T, Moschetta A, Lee YK, *et al*. Regulation of antibacterial defense in the small intestine by the nuclear bile acid receptor. *Proc Natl Acad Sci USA* 2006;103:3920–5.
50 Fang S, Suh JM, Reilly SM, *et al*. Intestinal FXR agonism promotes adipose tissue browning and reduces obesity and insulin resistance. *Nat Med* 2015;21: 159–65.

Figure S1. FXR does not contribute to increased lipogenesis in the liver. qPCR analysis of **A)** *Fas*, **B**) *Acc1*, **C)** *Pparα*, **D)** *Acox1* and **E)** *Cpta1* expression in livers from mice after 10 weeks on a HFD (n=4-9 mice per group). Mean values ± SEM are plotted; *p<0.05, **p<0.01, ***p<0.001 versus GF of same genotype; #significant for genotype-colonisation interaction.

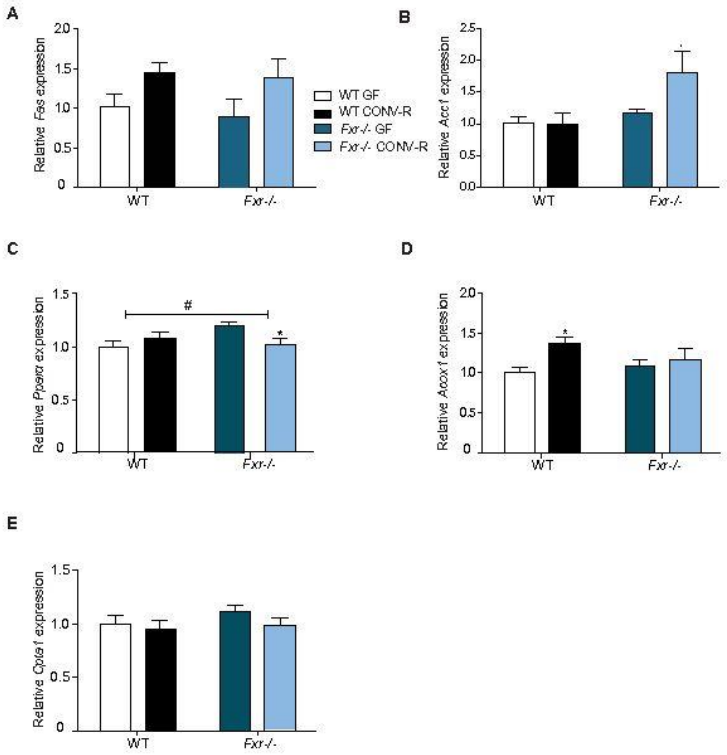

Parseus, Sommer et al; Figure 1, suppl

Figure S2. Bile acid profiles in serum from **A)** the vena cava (n=5-9 mice per group) and **B)** the caecum (n=4-9 mice per group) after 10 weeks on HFD. Mean values are plotted and p values determined by *t* test between CONV-R wild-type and *Fxr-/-* are listed. The following bile acids were analysed: TCA, taurocholic acid; TUDCA, tauroursodeoxycholic; TDCA, taurodeoxycholic acid; THDCA, taurohyodeoxycholic acid; DCA, deoxycholic acid; CA, cholic acid; TCDCA tauroconjugated chenodeoxycholic acid; T-ωMCA, tauroconjugated omega murocholic acid; T-αMCA, tauroconjugated alpha murocholic acid; T-βMCA, tauroconjugated beta murocholic acid; ωMCA, omega murocholic acid; αMCA, alpha murocholic acid; βMCA, beta murocholic acid; TLCA, taurolitocholic acid; UDCA, ursodeoxycholic acid and HDCA, hyodeoxycholic acid. Not all bile acids were detected and those undetected or at low levels (>1%) are combined as other.

A

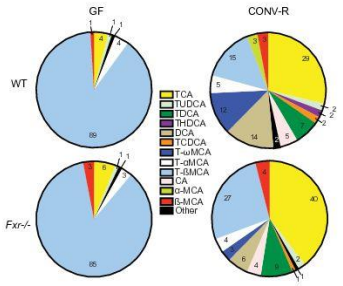

Calculated p-values (unpaired, two-tailed t test, FDR corrected) comparing relative serum levels of bile acids between CONV-R wildtype and *Fxr-/-* mice.

Groups	TCA	TUDCA	TDCA	THDCA	DCA	TCDCA	T-ωMCA	T-αMCA	T-βMCA	CA	αMCA	βMCA	HDCA	ωMCA
CONVR WT vs. CONVR *Fxr-/-*	0.30	0.77	0.58	0.03	0.14	0.39	0.03	0.20	0.04	0.59	0.28	0.59	0.05	0.39

B

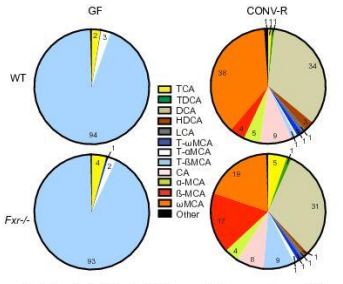

Calculated p-values (unpaired, two-tailed t test, FDR corrected) comparing relative caecum levels of bile acids between CONV-R wildtype and *Fxr-/-* mice.

Groups	TCA	TDCA	DCA	HDCA	LCA	T-ωMCA	T-αMCA	T-βMCA	CA	αMCA	βMCA	ωMCA
CONVR WT vs. CONVR *Fxr-/-*	0.28	0.66	0.91	0.24	0.91	0.92	0.66	0.24	0.92	0.91	0.07	0.21

Figure S3. qRT-PCR analysis of **A)** *Cyp7a1* and **B**) *Cyp8b1* expression in livers from GF and CONV-R wild-type and *Fxr-/-* mice after 10 weeks on HFD (n=4-9 mice per group). Mean values ± SEM are plotted; *p<0.05, **p<0.01, ***p<0.001 versus GF of same genotype; #significant for genotype-colonisation interaction.

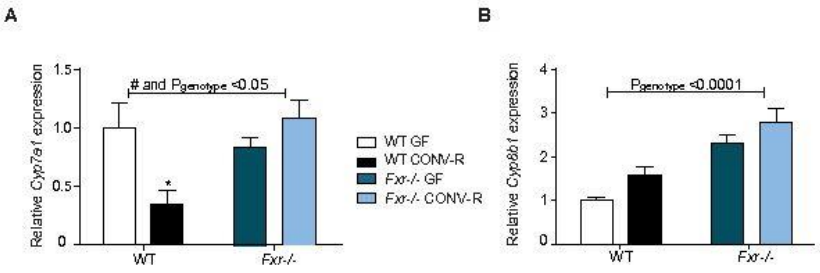

Table S1. Antibodies used for histology, related to Materials and Methods

Antibody	Application	primary/ secondary	raised in	dilution	Supplier
MAC-2/galectin-3	WAT	primary	Rat	1/500	Cedarlane Laboratories, #CL8942AP
rabbit biotinylated anti-rat	WAT	secondary	Rabbit	1/500	Vector laboratories, #VEBA-4001
Polyclonal Guinea Pig Anti-Insulin	pancreas	primary	Guinea pig	1/800	DAKO, #A0564
Biotinylated Goat Anti-Guinea Pig IgG Antibody	pancreas	secondary	Goat	1/800	Vector laboratories, #BA-7000

Table S2. Primer sequences for qRT-PCR

Gene	Abbreviation	Primer sequence
Acetyl-CoA carboxylase	*Acc1*	AAGTCCTTGGTCGGGAAGTATACA ACTCCCTCAAAGTCATCACAAACA
Acyl-CoA oxidase 1	*Acox1*	CCGCCACCTTCAATCCAGAG CAAGTTCTCGATTTCTCGACGG
Apolipoprotein C2/Apolipoprotein C-II	*Apoc2*	CCCTTCCTGCCACTACATTC CAACATCAGGATGACCAGGA
Cluster of differentiation 36/fatty acid translocase	*Cd36*	TTGTACCTATACTGTGGCTAAATGAGA CTTGTGTTTGAACATTTCTGCTT
Carnitine palmitoyltransferase 1A	*Cpt1a*	TGCCTCTATGTGGTGTCCAA TCAAACAGTTCCACCTGCTG
Cytochrome P450, family 7, subfamily A, polypeptide 1 (Cholesterol 7α- hydroxylase)	*Cyp7a1*	AGCAACTAAACAACCTGCCAGTACTA GTCCGGATATTCAAGGATGCA
Cytochrome P450, family 8, subfamily B, polypeptide 1 (Sterol 12α-hydroxylase)	*Cyp8b1*	GGCTGGCTTCCTGAGCTTATT ACTTCCTGAACAGCTCATCGG
EGF-like module-containing mucin-like hormone receptor-like 1	*Emr1*	GGAGGACTTCTCCAAGCCTATT AGGCCTCTCACTTCTGCTT
Fatty acid synthetase	*Fas*	TGGTGAATTGTCTCCGAAAAGA CACGTTCATCACGAGGTCATG
Peroxisome proliferator-activated receptor alpha	*Ppara*	CACGCATGTGAAGGCTGTAA GCTCCGATCACACTTGTCG
Scavenger receptor class B member 1	*Srb1*	CGTTGTCATGATCCTCATGTT ACAGGCTGCTCGGGTCTAT
Serum amyloid A 3	*Saa3*	TGCCATCATTCTTTGCATCTTGA CCGTGAACTTCTGAACAGCCT
Tumor necrosis factor α	*Tnfa*	CCAGACCCTCACACTCA CACTTG GTGGTTTGCTACGAC
Very-low-density-lipoprotein receptor	*Vldlr*	GCCCGTTCTACTCAGTGTATCC GAACTCATCTGCACTACATGTTATGTT

Table S3. 2-way ANOVA followed by Bonferroni post-tests, related to figures 1-3 and Supplementary figure 1

Figure 1	**B) Body weight after high fat diet**		**C) Fasting glucose**		**D) AUC, oral glucose tolerance test**	
Source of Variation	% of total variation	P value	% of total variation	P value	% of total variation	P value
Interaction	21,17	< 0,0001	0,06702	0,8239	0,4513	0,4689
Genotype (WT/*Fxr-/-*)	7,349	0,0105	45,14	< 0,0001	51,07	< 0,0001
Colonization (GF/CONV-R)	37,86	< 0,0001	26,41	0,0002	30,97	< 0,0001

Figure 1	**E) AUC, Insulin tolerance test**		**I) Beta cell mass**	
Source of Variation	% of total variation	P value	% of total variation	P value
Interaction	2,119	0,1618	12,85	0,05
Genotype (WT/ *Fxr-/-*)	42,07	< 0,0001	3,189	0,3128
Colonization (GF/CONV-R)	13,83	0,0008	17,92	0,0228

Figure 2	**B) Crown-like structures**		**C) *Emr1* mRNA levels**	
Source of Variation	% of total variation	P value	% of total variation	P value
Interaction	17,99	0,0058	15,59	0,0045
Genotype (WT/*Fxr-/-*)	3,03	0,2247	10,86	0,015
Colonization (GF/CONV-R)	32,38	0,0005	27,13	0,0004

Figure 2	**D) *Saa3* mRNA levels**		**E) *Tnfa* mRNA levels**	
Source of Variation	% of total variation	P value	% of total variation	P value
Interaction	15,22	0,0053	15,08	0,0362
Genotype (WT/*Fxr-/-*)	8,397	0,0311	1,289	0,5209
Colonization (GF/CONV-R)	36,51	< 0,0001	14,05	0,0425

Figure 3	**A) Triglycerides**		**B) Cholesteryl esters**		**C) ALT activity**	
Source of Variation	% of total variation	P value	% of total variation	P value	% of total variation	P value
Interaction	16,66	0,0007	8,914	0,1122	8,914	0,1122
Genotype (WT/*Fxr-/-*)	12,88	0,0023	11,68	0,0719	11,68	0,0719
Colonization (GF/CONV-R)	32,68	< 0,0001	19,35	0,024	19,35	0,024

Figure 3	**D) *Cd36* mRNA levels**		**E) *Apo-C II* mRNA levels**		**F) *Vldlr* mRNA levels**	
Source of Variation	% of total variation	P value	% of total variation	P value	% of total variation	P value
Interaction	10,76	0,0607	10,76	0,0607	6,446	0,068
Genotype (WT/*Fxr-/-*)	0,736	0,6096	0,736	0,6096	12,83	0,0127
Colonization (GF/CONV-R)	31,08	0,0029	31,08	0,0029	27,55	0,0006

Supp. Figure 1	**A) *Fas* mRNA levels**		**B) *ACC1* mRNA levels**	
Source of Variation	% of total variation	P value	% of total variation	P value
Interaction	0,09757	0,883	7,928	0,115
Genotype (WT/*Fxr-/-*)	1,053	0,6299	17,12	0,0245
Colonization (GF/CONV-R)	23,66	0,0327	7,33	0,1289

*All comparisons were made with 2-way ANOVA followed with post hoc Bonferroni post-tests.*p < 0.05, **p < 0.01, ***p <0.001.*